

Increased carnitine palmitoyl transferase 1 expression and decreased sterol regulatory element–binding protein 1c expression are associated with reduced intramuscular triglyceride accumulation after insulin therapy in high-fat–diet and streptozotocin-induced diabetic rats

Yan Bi¹, Mengyin Cai¹, Hua Liang¹, Weiping Sun, Xiubin Li, Chunxia Wang, Yanhua Zhu, Xiang Chen, Ming Li, Jianping Weng*

Department of Endocrinology, The Third Affiliated Hospital of Sun Yat-sen University, Guangzhou 510630, PR China

Received 19 August 2008; accepted 27 January 2009

Abstract

We previously reported that early insulin treatment reduced intramuscular triglyceride content in type 2 diabetes mellitus Sprague-Dawley rats; the underlying mechanisms are, however, not completely understood. Here we investigated the regulation of insulin on molecular expressions involved in lipid metabolism pathways in skeletal muscle of high-fat–diet and streptozotocin-induced diabetic Sprague-Dawley rats. Neutral protamine Hagedorn insulin and gliclazide were initiated at the third day after streptozotocin injection and lasted for 3 weeks. Compared with normal rats, untreated diabetic rats had a 30% and 61% increase in lipoprotein lipase protein expression and activity, which were decreased by insulin and gliclazide ($P < .05$). Fatty acid translocase protein was down-regulated by 45% in untreated diabetic rats, which was up-regulated by 31% and 26% with insulin and gliclazide, respectively ($P < .05$). Insulin failed to affect fatty acid transport protein 1 and fatty acid binding protein expressions. Carnitine palmitoyl transferase 1 had a 47% decrease in untreated diabetic rats, which was normalized by insulin ($P < .05$). Moreover, compared with normal rats, untreated diabetic rats had higher expressions of sterol regulatory element–binding protein 1c, tumor necrosis factor α , and Tyr⁷⁰⁵ phosphorylation of signal transducer and activator of transcription 3 levels, which all were down-regulated after insulin treatment. These results suggested that early insulin reduced intramuscular triglyceride levels in diabetic rats potentially through amelioration of lipid dysfunction and inhibition of lipid synthesis.

© 2009 Elsevier Inc. All rights reserved.

1. Introduction

Lipid accumulation in muscle can be interpreted as the consequence of increased supply of fatty acids and/or decreased oxidation of lipids and/or increased lipid synthesis [1,2].

Generally, circulating triglyceride is transported in the form of lipoprotein, which is hydrolyzed by lipoprotein lipase (LPL) for the delivery of fatty acids to muscle. Transgenic mice specifically overexpressing LPL in skeletal muscle caused elevated tissue triglyceride levels and insulin resistance [3],

suggesting that increased capacity for the transfer of lipids from triglyceride-rich lipoprotein particles to the muscle cells can be involved in muscle triglyceride content [4–6]. The next process regarding the uptake and movement of fatty acids into the cell is not fully understood, but seems to be involved in specific fatty acid transporters, including fatty acid translocase (FAT), fatty acid binding protein (FABP), and fatty acid transport protein 1 (FATP-1) [7]. Fatty acid translocase is abundantly expressed in tissues with high metabolic capacity for fatty acids. Transgenic mice overexpressing FAT in muscle showed an enhanced ability of muscle to oxidize fatty acids in response to stimulation and contraction, together with decreased triglyceride levels [8]. Other proposed mediators of fatty acids uptake are FABP and FATP-1, which were reported to be correlated with fatty acids utilization in a variety of different circumstances [7]. Fatty acids are taken up into the cells and may enter a triglyceride pool for temporary storage;

Part of this study was presented at the American Diabetes Association's 68th Scientific Sessions, San Francisco, CA, June 6–10, 2008.

* Corresponding author. Tel.: +86 2085252107; fax: +86 2085252107.

E-mail address: wjianp@mail.sysu.edu.cn (J.P. Weng).

¹ These authors contributed equally to the paper.

then their final fate will be oxidation. One step that may possibly be rate limiting for mitochondrial oxidation is the transport of fatty acids into mitochondria by means of carnitine palmitoyl transferase 1 (CPT-1) [9–11]. A study investigating the “in vitro” fat oxidation in muscle biopsies of obese subjects indicated that defect at CPT-1 level could contribute to the reduced lipid oxidation in human skeletal muscle [12,13]. Moreover, it was reported that hyperglycemia may lead to a reduction of CPT-1 activity and subsequently lower fatty acid oxidation, then shunting toward lipid accumulation [14].

Another possibility controlling intramuscular triglyceride (IMTG) deposition is through up-regulation of the de novo lipogenesis in skeletal muscle. Sterol regulatory element-binding protein 1c (SREBP-1c) is a critical transcriptional regulator of lipid biosynthesis and glucose metabolism in muscle, regulating gene expression of several enzymes including fatty acid synthase (FAS), acetyl-coenzyme A (CoA) carboxylase (ACC), and hexokinase II [15–17]. Expression of SREBP-1 in skeletal muscle is enhanced by insulin, and insulin deficiency leads to a decrease in SREBP-1 [18]. In addition, muscle SREBP-1c expression is also regulated by hyperglycemia and nutritional status [15,17]. Aberrant regulation of SREBP-1c might underlie the dyslipidemia that leads to lipid accumulation and insulin resistance in skeletal muscle [19,20].

Our previous studies showed that early insulin therapy in type 2 diabetes mellitus subjects [21,22] and animal models improved insulin resistance and decreased IMTG [23]; the underlying mechanisms are, however, not completely understood. The aim of the study was therefore to determine the in vivo regulation by insulin therapy of the expression of those proteins involved in fatty acid metabolism in skeletal muscle in the early stage of high-fat-fed, low-dose streptozotocin (STZ)-treated diabetic rat, a model that was characterized by mild hyperglycemia accompanied by insulin resistance without significant elevation in insulin levels [23].

2. Materials and methods

2.1. Type 2 diabetes mellitus rat model

The type 2 diabetes mellitus rat model was developed as previously described [23,24] using male Sprague-Dawley rats (7–8 weeks, approximately 200 g; Southern Medical University, Guangzhou, China). All procedures were in accordance with the principles of laboratory animal care (National Institutes of Health publication no. 85-23, revised 1985) and were approved by Sun Yat-sen University Animal Care and Use Committee. The rats were randomly assigned to normal diet (as a percentage of total kilocalories consisting of 10% fat, 64% carbohydrate, and 26% protein) or a high-fat diet (HFD) (consisting of 56% fat, 32% carbohydrate, and 14% protein). After 5 weeks, diabetes was induced in HFD rats by a single intraperitoneal injection of STZ (Sigma, St Louis, MO) at 40 mg/kg body weight (in 0.1 mol/L citrate-buffered saline, pH 4.2) after an overnight fast. The control

rats were fasted in an identical manner and had a volume of citrate-buffered saline, equal to that of the STZ solution, injected by the same route. All animals continued on their original diets for the duration of the study.

2.2. Treatment protocol

Treatment protocol had been described previously [23]. Briefly, the intervention study was initiated from the third day after STZ injection. Weight- and glucose-matched rats were further divided randomly into 4 groups of 6 animals each, as follows:

NC group: normal control.

DM group: untreated diabetic rats during the intervention study.

INS group: diabetic rats treated with neutral protamine Hagedorn (NPH) insulin for 3 weeks from third day after STZ injection.

GLI group: diabetic rats treated with gliclazide for 3 weeks from third day after STZ injection.

Rats were given NPH insulin (6–8 U/d, subcutaneous) or gliclazide (80 mg/[kg d], oral gavage) for a total of 3 weeks in the intervention study. The doses of NPH insulin and gliclazide were based on the preliminary study to reduce nonfasting glucose concentration to less than 8 mmol/L in a week. After the completion of treatment, all animals were maintained on their previous diet for 3 days. Rats were anesthetized, and tissue samples from skeletal muscle were removed from both control and treated animals. Tissues were flash frozen in liquid nitrogen and stored at -80°C for further analysis.

2.3. Biochemical analysis

Fasting blood was sampled from tail vein after overnight fast. Blood glucose levels were tested by glucometer (Roche, Basel, Switzerland) with samples run in duplicate, and serum insulin levels were measured by radioimmunoassay using a commercial kit (Linco Research, Missouri, USA) with intraassay coefficient of variance less than 5.0%. Serum levels of triglyceride and total cholesterol as well as hemoglobin A_{1c} (HbA_{1c}) were detected using automatic biochemistry analyzer.

For measurement of glucose-insulin index, an intraperitoneal glucose tolerance test was performed 48 hours after the end of intervention. Baseline glucose levels were determined after a 12-hour fast, after which glucose (1.5 g/kg body weight) was administered intraperitoneally to nonsedated animals. Tail blood samples were taken at 0 (before glucose administration), 30, and 120 minutes after administration of glucose. The glucose-insulin index was calculated as the area under the glucose and insulin curve (AUC), which is an indirect index of peripheral insulin action on glucose disposal.

Skeletal muscle triglycerides were extracted and measured as described previously [23]. After dissecting any visible adipose tissue, 100 mg of tissue was weighed and

homogenized in a handheld tissue homogenizer using a volume of ice-cold chloroform-methanol (2:1, vol/vol) 5 times the tissue weight. Triglycerides were extracted during 5 hours of shaking at room temperature. For phase separation, chloroform was added, samples were centrifuged, and the organic bottom layer was collected. The organic solvent was dried and dissolved in chloroform. Triglyceride content of each sample was measured in duplicate by use of an enzymatic method.

2.4. Preparation of nuclear and cytoplasmic extracts

After dissecting any visible adipose tissue, 100 mg of muscle tissue was ground in a liquid nitrogen-cooled mortar and pestle with lysis buffer. Nuclear and cytoplasmic proteins were extracted as per manufacturer's recommendations (Pierce, Rockford, IL, USA). All centrifugation steps were performed at 4°C, and all cell samples and extracts were kept on wet ice during the procedure. Protein concentration was quantified using the bicinchoninic acid protein assay method. Nuclear and cytoplasmic fractions were stored at –80°C until used.

2.5. Western blot analysis

Nuclear protein (80 µg) and cytoplasmic protein (120 µg) were separated by sodium dodecyl sulfate–polyacrylamide gel electrophoresis on 10% polyacrylamide gels and transferred to nitrocellulose. The membranes were blocked for 2 hours at room temperature with 5% nonfat milk in Tris-buffered saline containing 0.1% Tween 20. The specific antibodies to SREBP-1, LPL, FATP-1, FABP, FAT, CPT-1, tumor necrosis factor α (TNF- α), and phospho-signal transducer and activator of transcription 3 (STAT3) (Tyr⁷⁰⁵) (all from Santa Cruz Biotechnology, Santa Cruz, CA) were diluted in 1:500 and incubated overnight at 4°C. For Sp3 and glyceraldehyde-3-phosphate dehydrogenase (GAPDH) (all from eBioscience, San Diego, CA, USA), specific antibodies were diluted in 1:1000 and incubated overnight. The membranes were then washed for 30 minutes using Tris-buffered saline containing 0.1% Tween 20, followed by 1

hour of incubation with peroxidase-conjugated secondary antibodies (1:2000; Boster, Wuhan, China); proteins were visualized using the luminol reagent (Santa Cruz Biotechnology). Band intensities were quantified by densitometry.

2.6. RNA isolation from rat skeletal tissue

Total RNA was extracted from frozen tissues using standard Trizol RNA isolation method. The purity and quality of RNA were assessed using the DU640 nucleic acid analyzer (Beckman, California, USA). RNA was visualized using ethidium bromide and a 0.24- to 9.5-kilobase RNA ladder to verify lack of degradation.

2.7. Quantitative real-time reverse transcriptase polymerase chain reaction

Reverse transcription of 5 µg RNA was carried out according to the instructions of SuperScript III First-Strand Synthesis System for reverse transcriptase polymerase chain reaction (PCR) (Invitrogen Life Science, California, USA). Real-time PCR quantified amplifications of complementary DNA with both sense and antisense oligonucleotides at a final volume of 20 µL using the SYBR green TaqMan Universal PCR Master Mix (Toyobo, Osaka, Japan), and results were normalized against β -actin gene expression. Primer sequences were as follows: rat SREBP-1c forward primer (5'-GCAACACTGGCAGAGATCTACGT-3'), rat SREBP-1c reverse primer (5'-TGGCGGGCACTACTTAG-GAA-3'), rat β -actin forward primer (5'-GGAGAT-TACTGCCCTGGCTCCTA-3'), and rat β -actin reverse primer (5'-GACTCATCGTACTCCTGCTTGCTG-3').

2.8. Colorimetry method for determining LPL activity

The activities of LPL were detected by colorimetric method (Jiancheng Bioscience Technology, Nanjing, China). The LPL could hydrolyze the triglyceride in intralipid into glycerine and free fatty acid. By determining the amount of free fatty acid by copper-reagent method and protein concentration, we could measure the activities of LPL.

Table 1
Characteristics of the experimental animals after 48 hours at the end of intervention study

	NC	DM	INS	GLI
Body weight (g)	489 ± 22	464 ± 26	486 ± 38	459 ± 27
Fasting blood glucose (mmol/L)	4.73 ± 0.81	23.8 ± 3.91*	9.63 ± 1.50*,§	10.63 ± 1.46 ^{†,‡}
Insulin (ng/mL)	0.67 ± 0.20	0.59 ± 0.25	0.69 ± 0.23	0.72 ± 0.27
HbA _{1c} (%)	4.17 ± 0.82	7.70 ± 1.04 [†]	6.02 ± 1.55*,‡	6.40 ± 0.35*,‡
Cholesterol (mmol/L)	1.91 ± 0.39	2.17 ± 0.47	1.62 ± 0.40	1.90 ± 0.29
Triglyceride (mmol/L)	1.05 ± 0.74	3.69 ± 0.73 [†]	1.75 ± 0.48 [‡]	1.99 ± 1.17 [‡]
Muscle triglyceride (mmol/L)	0.29 ± 0.11	0.98 ± 0.08*	0.49 ± 0.09*,‡	0.52 ± 0.06*,‡
Glucose AUC (mmol/L × min)	607.4 ± 378.2	2880.5 ± 365.8 [†]	2187.0 ± 351.9 ^{†,§}	2394.6 ± 143.2 ^{†,§}
Insulin AUC (ng/mL × min)	55.2 ± 12.9	34.8 ± 1.2 [†]	37.2 ± 5.9*	34.4 ± 2.0 [†]
Glucose-insulin index (U × 10 ³)	49.9 ± 8.0	103.7 ± 13.7*	82.3 ± 8.9*,‡	85.2 ± 9.0*,‡

Data are given as mean ± SD, and assays were performed on 4 to 6 animals in each group.

**P* less than .05 and [†]*P* less than .01 compared with values for normal control rats.

[‡]*P* less than .05 and §*P* less than .01 compared with values for diabetic rats with no therapy.

2.9. Statistical analysis

The results are expressed as the means \pm SD. A *t* test or analysis of variance was used to determine statistical significance, with a *P* value less than .05 considered statistically significant.

3. Results

3.1. Characteristics of the experimental animals

Body weight and nonfasting glucose during the intervention study are shown in Table 1 and Fig. 1. There were no significant differences in body weights among groups (Table 1). Pretreatment nonfasting blood glucose levels were 5.1 mmol/L in the NC group and 22 to 24 mmol/L in all diabetic groups. Insulin and gliclazide treatment each significantly reduced blood glucose levels after 1 week and maintained them throughout the treatment, although the levels remained higher than those in normal rats (Fig. 1).

The characteristics of experimental animals 48 hours after the end of intervention study are shown in Table 1. Diabetic rats exhibited obviously disturbed metabolism, indicated by elevated HbA_{1c} levels and fasting blood glucose levels, as well as elevated triglyceride levels ($P < .01$). In addition, diabetic rats had 3.38-fold increases in muscle triglyceride ($P < .01$). Serum fasting insulin levels were comparable with those in normal control rats. Insulin treatment modified HbA_{1c} levels, fasting blood glucose, and muscle triglyceride contents ($P < .05$), although they remained higher than those in normal rats. Likewise, gliclazide treatment resulted in significant reduction in triglyceride, HbA_{1c}, fasting blood glucose, and muscle triglyceride contents ($P < .05$).

An intraperitoneal glucose tolerance test done 48 hours after the end of the early intervention study showed that the glucose-insulin index increased by 2.5-fold in diabetic rats compared with normal rats (Table 1). During 3 weeks of

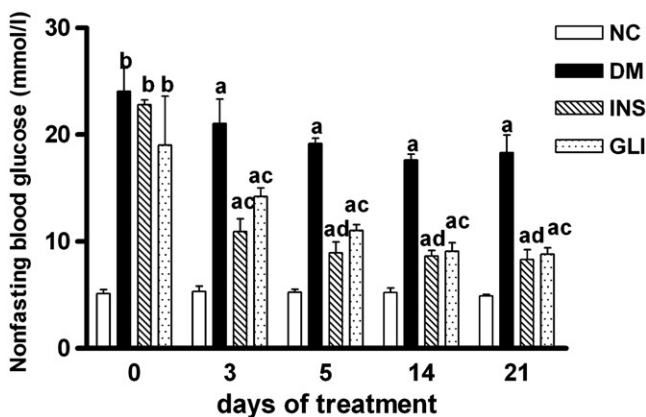


Fig. 1. Nonfasting blood glucose levels during intervention studies. Data are means \pm SD; *n* = 4 to 6 rats per group. ^a*P* less than .05 and ^b*P* less than .01 compared with values for normal control rats. ^c*P* less than .05 and ^d*P* less than .01 compared with values for diabetic rats with no therapy.

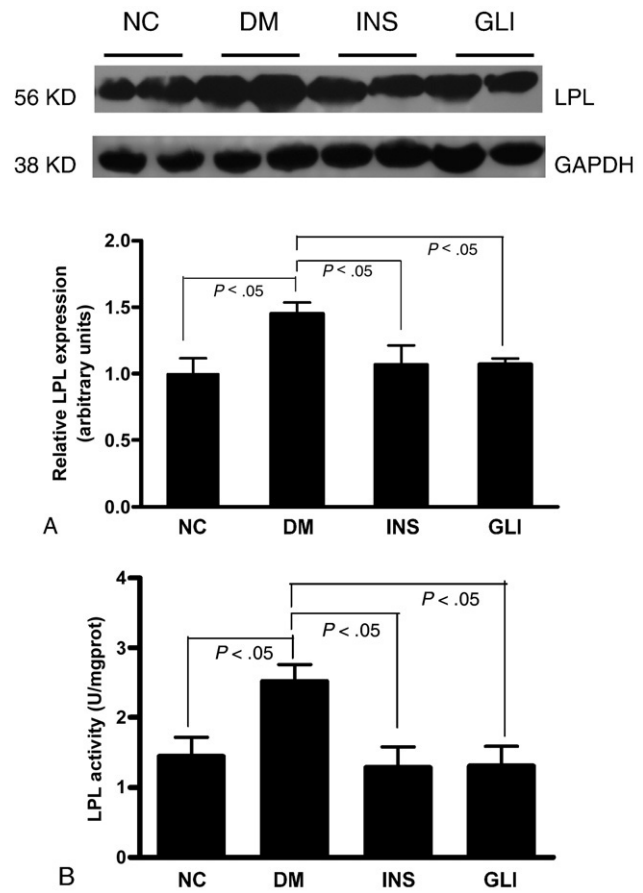


Fig. 2. Effects of 3-week intervention on LPL protein levels in Western blot (A) and LPL activities (B) in colorimetry in muscle. The bars represent means \pm SD for 4 to 6 rats per group. The intensity of the bands in Western blot was quantified by densitometric analysis and normalized with corresponding GAPDH.

early insulin treatment, the glucose-insulin index was reduced by nearly 33% relative to their untreated diabetic counterparts, although it was still higher than that in normal rats. Similarly, early gliclazide-treated diabetic rats had reduced levels of the glucose-insulin index by about 27% relative to the values from untreated diabetic rats.

3.2. Insulin and gliclazide decreased LPL protein and activity

Lipoprotein lipase is the rate-limiting process for hydrolysis; we assessed the effects of insulin treatment on LPL protein expressions (Fig. 2A) and LPL activities (Fig. 2B). Compared with control, untreated diabetic rats had a 30% and 61% increase in LPL protein content and LPL activity, which were significantly decreased by insulin and gliclazide treatment ($P < .05$).

3.3. Insulin and gliclazide increased FAT protein

Fatty acid translocase, FABP, and FATP-1 are 3 proteins involved in fatty acid uptake. Compared with control, the abundance of FAT protein in the untreated diabetic rats was

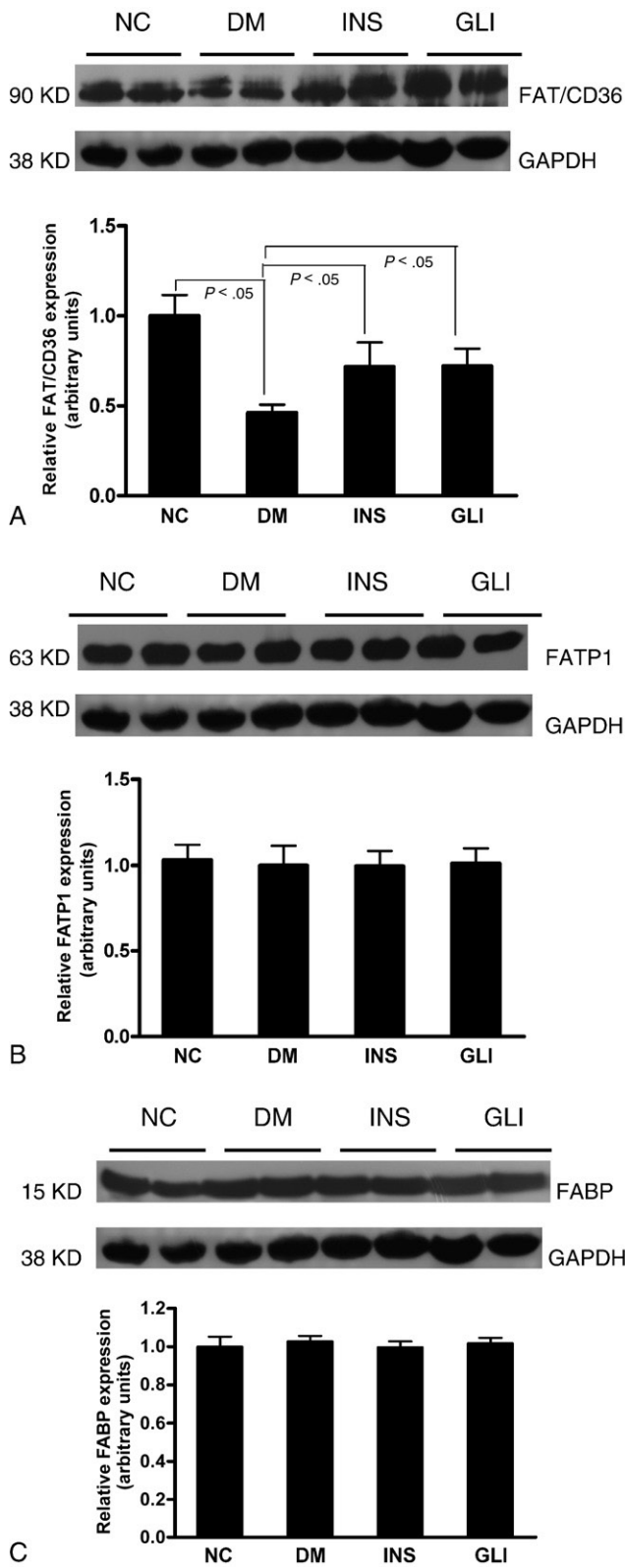


Fig. 3. Effects of 3-week intervention on FAT/CD36 (A), FATP-1 (B), and FABP (C) levels in Western blot in muscle. The bars represent means \pm SD for 4 to 6 rats per group. The intensity of the bands was quantified by densitometric analysis and normalized with corresponding GAPDH.

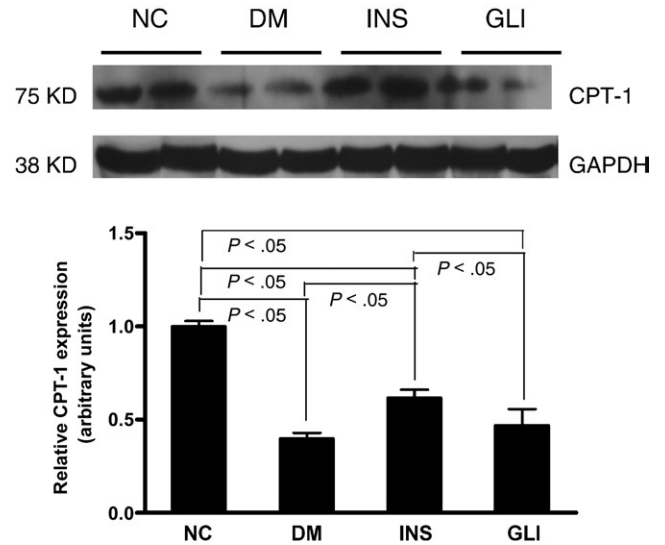


Fig. 4. Effects of 3-week intervention on CPT-1 protein levels in Western blot in muscle. The bars represent means \pm SD for 4 to 6 rats per group. The intensity of the bands was quantified by densitometric analysis and normalized with corresponding GAPDH.

decreased by 45%, which was increased by 31% and 26% by insulin and gliclazide, respectively ($P < .05$, Fig. 3A). Insulin and gliclazide had no significant impact on FATP-1 (Fig. 3B) and FABP protein levels (Fig. 3C).

3.4. Insulin increased CPT-1 protein

Carnitine palmitoyl transferase 1 is a rate-limiting step that contributes to fat oxidation; we assessed the effect of treatment on CPT-1 protein level by immunoblotting. Compared with controls, CPT-1 protein level in the untreated diabetic rats was decreased by 47%. Early insulin treatment increased CPT-1 protein level by 57.5% compared with that in untreated diabetic rats, whereas gliclazide treatment failed

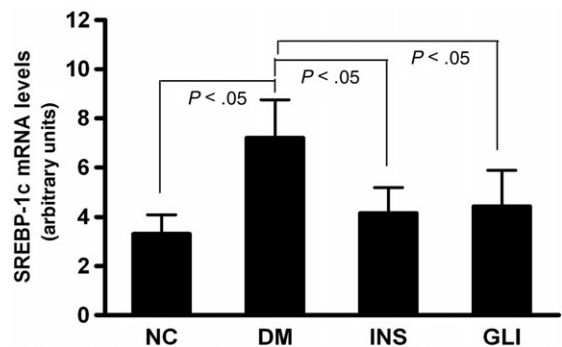


Fig. 5. Effects of 3-week intervention on the expression of SREBP-1c mRNA. Rat gastrocnemius muscle was harvested at the time of killing, and mRNA was harvested as described in the "Materials and methods" section. Results are plotted as the means \pm SD ($n = 6$ per group). Quantitative real-time PCR for SREBP-1c mRNA: β -actin mRNA was used as a control, and results are expressed as relative units (SREBP-1c mRNA/ β -actin mRNA).

to affect CPT-1 expression ($P < .05$, Fig. 4). Stepwise logistic analysis showed correlation between CPT-1 protein with IMTG ($\gamma = -0.678$, $P < .01$).

3.5. Insulin and gliclazide decreased SREBP-1c messenger RNA

As SREBP-1c is the isoform most related to lipogenesis in vivo, we assessed the effect of treatment on gastrocnemius SREBP-1c messenger RNA (mRNA) levels using quantitative real-time PCR (Fig. 5). Sterol regulatory element-binding protein 1c mRNA level in diabetic muscle was increased by 2.14-fold. Insulin and gliclazide significantly reduced SREBP-1c mRNA levels compared with those of untreated diabetic rats ($P < .05$).

3.6. Insulin and gliclazide decreased nuclear mature SREBP-1c protein

Activation of SREBP-1 requires cleavage and entry of the mature protein into the nucleus. Therefore, we used immunoblotting to determine the protein level of nuclear mature SREBP-1c (Fig. 6). Compared with controls, diabetic

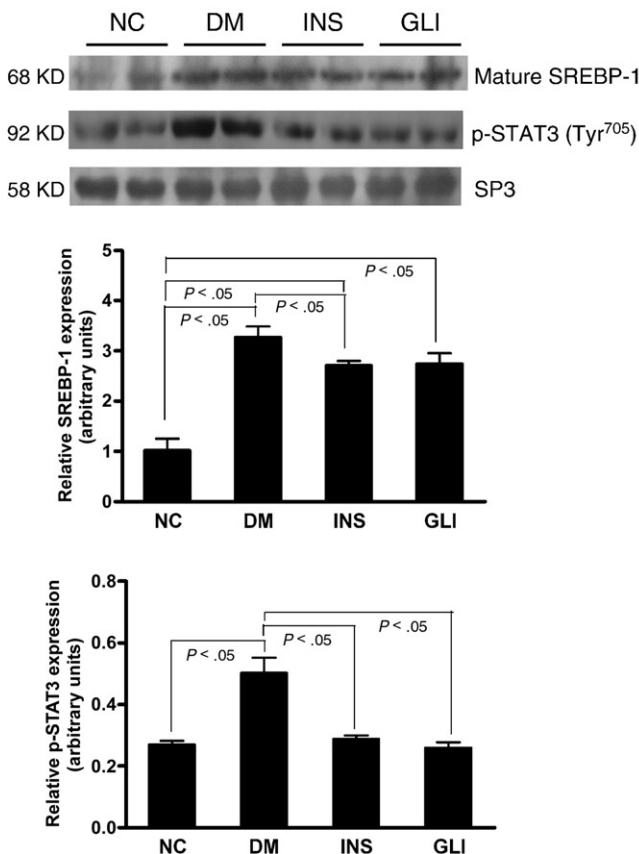


Fig. 6. Effects of 3-week intervention on nuclear mature SREBP-1 protein and Tyr⁷⁰⁵ phosphorylation of STAT3 protein levels in Western blot in muscle. The bars represent means \pm SD for 4 to 6 rats per group. The intensity of the bands was quantified by densitometric analysis and normalized with corresponding Sp3.

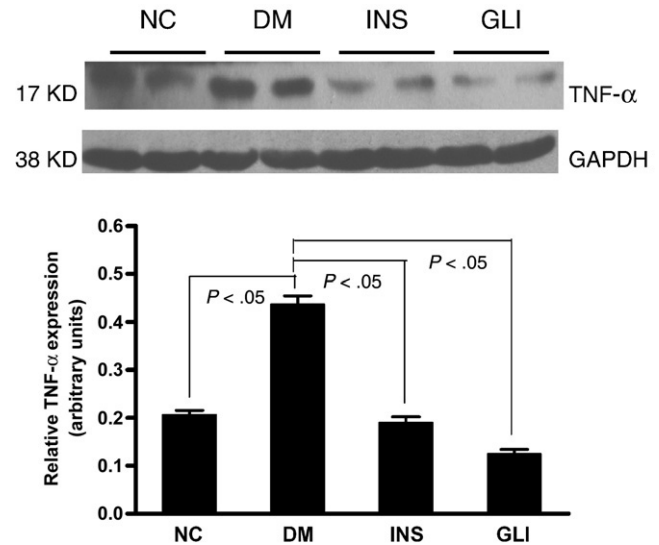


Fig. 7. Effects of 3-week intervention on TNF- α protein levels in Western blot in muscle. The bars represent means \pm SD for 4 to 6 rats per group. The intensity of the bands was quantified by densitometric analysis and normalized with corresponding GAPDH.

rats had a 2.45-fold increase in mature SREBP-1 protein content in muscle. Insulin and gliclazide significantly decreased mature SREBP-1 protein in the gastrocnemius compared with that in untreated diabetic rats, although it was still higher than that in normal control rats ($P < .05$). Stepwise logistic analysis showed correlation between SREBP-1c protein with IMTG ($\gamma = 0.754$, $P < .01$).

3.7. Insulin and gliclazide decreased phosphorylation of STAT3 protein

Signal transducer and activator of transcription 3 protein was a cytoplasmic-signal-dependent transcription factor that was phosphorylated by Janus kinase protein; phosphorylated STATs form dimers, enter the nucleus, and regulate gene transcription. It had been reported that Tyr⁷⁰⁵ phosphorylation of STAT3 was involved in glucose-induced up-regulation of SREBP-1c expression. Therefore, we analyzed the expression of nuclear Tyr⁷⁰⁵ phosphorylation of STAT3. Compared with controls, diabetic rats had an increase in p-STAT3 (Tyr⁷⁰⁵) protein abundance (Fig. 6). Early insulin and gliclazide treatment significantly reduced expressions of p-STAT3 (Tyr⁷⁰⁵) compared with those in untreated diabetic rats ($P < .05$).

3.8. Insulin and gliclazide decreased TNF- α protein

Tumor necrosis factor α was reported to stimulate the maturation of SREBP-1; here we assessed the expression of TNF- α . Compared with controls, diabetic rats had a 2-fold increase in TNF- α protein abundance in muscle (Fig. 7). Early insulin and gliclazide treatment significantly reduced expressions of TNF- α compared with those in untreated diabetic rats ($P < .05$).

4. Discussion

Our study was undertaken as a first step to investigate the underlying molecular mechanisms involved in reduced fat accumulation in skeletal muscle, which is not generally regarded as having a high lipogenetic capacity, in response to insulin therapy. We found reduced IMTG accumulation after insulin therapy potentially resulting from both increased lipid oxidation and decreased lipid synthesis in the early stage of high-fat-fed, low-dose STZ-treated diabetic rat. Although there is limitation to our experiment because the model is relevant to only a specific stage in the course of type 2 diabetes mellitus and we do not measure fluxes through fat oxidation and lipogenesis, for which further work should be done in the future to give a functional data, the study still presents some potentially interesting insight into the mechanism of the reduction in IMTG when insulin is administered in the early phase of diabetes.

The current results suggested that insulin treatment might increase fatty acid uptake into muscle cells through up-regulation of FAT expression. How then did this observation coexisted with the ability of insulin to decrease IMTG content? A similar situation occurred when endurance training athletes showed increased triglyceride localization around the mitochondria yet did not display insulin resistance; an increased oxidative capacity of skeletal muscle in these individuals might provide a protective effect [25]. Indeed, our study showed that CPT-1 expression was elevated after insulin treatment. Nevertheless, the mechanisms responsible for such unexpected observation are not completely understood because insulin is reported to activate ACC2 (catalyzing the carboxylation of acetyl-CoA to malonyl-CoA), hence increasing malonyl-CoA and reducing CPT-1 activity [26–28]. Instead, alterations in FAT protein seemed more than adequate to explain observed changes in CPT-1 content. Recent information suggests that CPT-1 may not act alone in the regulation of fatty acyl-CoA entry into the mitochondria. Studies have demonstrated that FAT plays an important role in regulating fatty acid oxidation [29]. By use of immunoprecipitation techniques in rodent muscle, it was found that mitochondrial FAT was associated with CPT-1, demonstrating that mitochondrial FAT (in cooperation with CPT-1) may be an important mediator of fatty acid oxidation [30]. Because abnormalities in FAT have an impact on mitochondrial oxidation, we hypothesized that the increase in the abundance of FAT after insulin treatment may subsequently facilitate the enhanced CPT-1 expression.

Another potential mechanism controlling IMTG content is the lipogenetic pathway in muscle. Studies had identified SREBP-1c as a crossroad of physiologic and pathophysiologic lipid homeostasis [31]. However, evidence was emerging that the expression and regulation of SREBP-1c in muscle were altered. It was reported that SREBP-1c mRNA in skeletal muscle was slightly decreased in STZ-

induced type 1 diabetes mellitus animal model and in type 2 diabetes mellitus patients and was increased or not altered by insulin in rat primary myotubes and in individuals with type 2 diabetes mellitus [18,32,33]. Different from these studies, our study suggested that increased expression of SREBP-1c in skeletal muscles was in parallel with IMTG storage in type 2 diabetes mellitus rats. Moreover, the expression of SREBP-1c was decreased by insulin therapy targeting euglycemia. Previous studies showed that the compensatory hyperinsulinemia of insulin resistance increased SREBP-1c in multiple tissues; insulin was thus considered as a likely “culprit” [18,32,33]. However, as our study demonstrated, insulin level did not increase in diabetic rat [23]. Based on the characteristics of our model, we postulated that hyperglycemia, not insulin or hyperinsulinemia, might be possible contributor. High glucose could induce activation of SREBP-1c through Janus kinase/STAT3 pathway and up-regulate lipogenetic enzymes; subsequently, it might start a vicious circle of lipogenesis leading to lipotoxicity and insulin resistance [17]. In addition, other studies had indicated that TNF- α could result in the increased rates of fatty acid synthesis and activation of SREBP-1c in human hepatocytes; moreover, TNF- α was capable of inducing SREBP-1 maturation in a time- and dose-dependent manner [34,35]. Consistent with this, our previous and current studies showed that TNF- α expression was up-regulated in skeletal muscle from HFD- and STZ-induced type 2 diabetes mellitus rats [23]. Together, although the direct evidence for the mechanisms of the activation of SREBP-1c is not clear at the present time, TNF- α and STAT3 might be involved in the regulation of SREBP-1c in skeletal muscle from type 2 diabetes mellitus rat. We must emphasize that the unexpected observations have a close relationship with the early course of disease, where the different effects of various interventions on IMTG had been observed [23].

Taken together, our results supported that fatty acid oxidation and de novo lipogenesis had evolved as highly integrated processes [20]. Sterol regulatory element-binding protein 1c might be viewed as a possible cross talk between pathways to establish energy fluxes in skeletal muscle under pathophysiologic state. As shown in recent studies, activation of SREBP-1c by high glucose increased the expression of ACC2 and FAS, then leading to both decreased fatty acid oxidation and increased lipogenesis [17,20]. Furthermore, LPL was also reported to be up-regulated by SREBP-1c [36]. Thus, we tentatively hypothesize that inhibition of SREBP-1c expression might result in down-regulation of fatty acid storage as well as up-regulation of fatty acid oxidation for efficient use of fuels in skeletal muscle of diabetic state by early insulin therapy.

In summary, early insulin reduced IMTG levels in type 2 diabetes mellitus rats potentially through amelioration of mitochondrial dysfunction and inhibition of lipogenesis. A further understanding of the molecular mechanisms on reduction of IMTG content will help elucidate a new therapeutic target for the treatment of type 2 diabetes mellitus.

Acknowledgment

This work was supported by grants from National Basic Research Program of China (973 program: 2006 CB503902) and National Natural Science Foundation of China Grant Award (30800539).

References

- [1] Savage DB, Petersen KF, Shulman GI. Mechanisms of insulin resistance in humans and possible links with inflammation. *Hypertension* 2005;45:828–33.
- [2] Krebs M, Roden M. Molecular mechanisms of lipid-induced insulin resistance in muscle, liver and vasculature. *Diabetes Obes Metab* 2005;7:621–32.
- [3] McGarry JD. Banting lecture 2001: dysregulation of fatty acid metabolism in the etiology of type 2 diabetes. *Diabetes* 2002;51:7–18.
- [4] Preiss-Landl K, Zimmermann R, Hammerle G, et al. Lipoprotein lipase: the regulation of tissue specific expression and its role in lipid and energy metabolism. *Curr Opin Lipidol* 2002;13:471–81.
- [5] Voshol PJ, Jong MC, Dahlmans VE, et al. In muscle-specific lipoprotein lipase–overexpressing mice, muscle triglyceride content is increased without inhibition of insulin-stimulated whole-body and muscle-specific glucose uptake. *Diabetes* 2001;50:2585–90.
- [6] Kim JK, Fillmore JJ, Chen Y, et al. Tissue-specific overexpression of lipoprotein lipase causes tissue-specific insulin resistance. *Proc Natl Acad Sci U S A* 2001;98:7522–7.
- [7] Blaak EE. Fatty acid metabolism in obesity and type 2 diabetes mellitus. *Proc Nutr Soc* 2003;62:753–60.
- [8] Henry RR, Ciaraldi TP, Abrams-Carter L, et al. Glycogen synthase activity is reduced in cultured skeletal muscle cells of non–insulin-dependent diabetes mellitus subjects. *J Clin Invest* 1996;98:1231–6.
- [9] Kelley DE, Mandarino LJ. Fuel selection in human skeletal muscle in insulin resistance: a reexamination. *Diabetes* 2000;49:677–83.
- [10] Petersen KF, Dufour S, Befroy D, et al. Impaired mitochondrial activity in the insulin-resistant offspring of patients with type 2 diabetes. *N Engl J Med* 2004;350:664–71.
- [11] Petersen KF, Befroy D, Dufour S, et al. Mitochondrial dysfunction in the elderly: possible role in insulin resistance. *Science* 2003;300:1140–2.
- [12] Simoneau JA, Veerkamp JH, Turcotte LP, et al. Markers of capacity to utilize fatty acids in human skeletal muscle: relation to insulin resistance and obesity and effects of weight loss. *FASEB J* 1999;13:2051–60.
- [13] Kim JY, Hickner RC, Cortright RL, et al. Lipid oxidation is reduced in obese human skeletal muscle. *Am J Physiol Endocrinol Metab* 2000;279:E1039–44.
- [14] Rasmussen BB, Holmback UC, Volpi E, et al. Malonyl coenzyme A and the regulation of functional carnitine palmitoyltransferase–1 activity and fat oxidation in human skeletal muscle. *J Clin Invest* 2002;110:1687–93.
- [15] Tsintzas K, Jewell K, Kamran M, et al. Differential regulation of metabolic genes in skeletal muscle during starvation and refeeding in humans. *J Physiol* 2006;575:291–303.
- [16] Gosmain Y, Dif N, Berbe V, et al. Regulation of SREBP-1 expression and transcriptional action on HKII and FAS genes during fasting and refeeding in rat tissues. *J Lipid Res* 2005;46:697–705.
- [17] Guillet-Deniau I, Pichard AL, Kone A, et al. Glucose induces de novo lipogenesis in rat muscle satellite cells through a sterol-regulatory-element-binding-protein-1c–dependent pathway. *J Cell Sci* 2004;117:1937–44.
- [18] Guillet-Deniau I, Mieulet V, Le Lay S, et al. Sterol regulatory element binding protein–1c expression and action in rat muscles: insulin-like effects on the control of glycolytic and lipogenic enzymes and UCP3 gene expression. *Diabetes* 2002;51:1722–8.
- [19] Commerford SR, Peng L, Dube JJ, et al. In vivo regulation of SREBP-1c in skeletal muscle: effects of nutritional status, glucose, insulin, and leptin. *Am J Physiol Regul Integr Comp Physiol* 2004;287:R218–27.
- [20] Slawik M, Vidal-Puig AJ. Lipotoxicity, overnutrition and energy metabolism in aging. *Ageing Res Rev* 2006;5:144–64.
- [21] Li Y, Xu W, Liao Z, et al. Induction of long-term glycemic control in newly diagnosed type 2 diabetic patients is associated with improvement of beta-cell function. *Diabetes Care* 2004;27:2597–602.
- [22] Weng J, Li Y, Xu W, et al. Effect of intensive insulin therapy on beta-cell function and glycaemic control in patients with newly diagnosed type 2 diabetes: a multicentre randomised parallel-group trial. *Lancet* 2008;371:1753–60.
- [23] Bi Y, Sun WP, Chen X, et al. Effect of early insulin therapy on nuclear factor kappaB and cytokine gene expressions in the liver and skeletal muscle of high-fat diet, streptozotocin-treated diabetic rats. *Acta Diabetol* 2008;45:167–78.
- [24] Reed MJ, Meszaros K, Entes LJ, et al. A new rat model of type 2 diabetes: the fat-fed, streptozotocin-treated rat. *Metabolism* 2000;49:1390–4.
- [25] Goodpaster BH, He J, Watkins S, et al. Skeletal muscle lipid content and insulin resistance: evidence for a paradox in endurance-trained athletes. *J Clin Endocrinol Metab* 2001;86:5755–61.
- [26] Prentki M, Joly E, El-Assaad W, et al. Malonyl-CoA signaling, lipid partitioning, and glucolipotoxicity: role in beta-cell adaptation and failure in the etiology of diabetes. *Diabetes* 2002;51:S405–13.
- [27] Kim JA, Wei Y, Sowers JR. Role of mitochondrial dysfunction in insulin resistance. *Circ Res* 2008;102:401–14.
- [28] Liu HY, Zheng G, Zhu H, Woldegiorgis G. Hormonal and nutritional regulation of muscle carnitine palmitoyltransferase I gene expression in vivo. *Arch Biochem Biophys* 2007;465:437–42.
- [29] Schenk S, Horowitz JF. Coimmunoprecipitation of FAT/CD36 and CPT I in skeletal muscle increases proportionally with fat oxidation after endurance exercise training. *Am J Physiol Endocrinol Metab* 2006;291:E254–60.
- [30] Campbell SE, Tandon NN, Woldegiorgis G, et al. A novel function for fatty acid translocase (FAT)/CD36: involvement in long chain fatty acid transfer into the mitochondria. *J Biol Chem* 2004;279:36235–41.
- [31] Raghow R, Yellaturu C, Deng X, et al. SREBPs: the crossroads of physiological and pathological lipid homeostasis. *Trends Endocrinol Meta* 2008;19:65–73.
- [32] Ducluzeau PH, Perretti N, Laville M, et al. Regulation by insulin of gene expression in human skeletal muscle and adipose tissue. Evidence for specific defects in type 2 diabetes. *Diabetes* 2001;50:1134–42.
- [33] Nadeau KJ, Leitner JW, Gurerich I, et al. Insulin regulation of sterol regulatory element–binding protein–1 expression in L-6 muscle cells and 3T3 L1 adipocytes. *J Biol Chem* 2004;279:34380–7.
- [34] Sewter C, Berger D, Considine RV, et al. Human obesity and type 2 diabetes are associated with alterations in SREBP1 isoform expression that are reproduced ex vivo by tumor necrosis factor–alpha. *Diabetes* 2002;51:1035–41.
- [35] Lawler Jr JF, Yin M, Diehl AM, et al. Tumor necrosis factor–alpha stimulates the maturation of sterol regulatory element binding protein–1 in human hepatocytes through the action of neutral sphingomyelinase. *J Biol Chem* 1998;273:5053–9.
- [36] Schoonjans K, Gelman L, Haby C, et al. Induction of LPL gene expression by sterols is mediated by a sterol regulatory element and is independent of the presence of multiple E boxes. *J Mol Biol* 2000;304:323–34.